Deformation and hydrofracture in a subduction thrust at seismogenic depths: The Rodeo Cove thrust zone, Marin Headlands, California

Francesca Meneghini[†]
Dipartimento di Scienze della Terra, Università di Pisa, 53 Via S. Maria, Pisa 56126, Italy

J. Casey Moore
Earth and Planetary Sciences Department, University of California, 1156 High Street, Santa Cruz, California 96054, USA

ABSTRACT

We have investigated the fabric and the deformational processes of an exhumed subduction zone thrust active at seismogenic depths. The Rodeo Cove thrust zone, which outcrops north of the Golden Gate Bridge of San Francisco, imbricates two basalt-chert-sandstone sequences belonging to the Marin Headlands terrane (Franciscan Complex). The thrust outcrop is a 200-m-thick complex zone that displays a range of stratal disruption from incipient deformation to a broken formation in the central part of the outcrop, dominated by basaltic lithologies, where zones of concentration of deformation have been mapped. Disruption is made by variably dense discrete fault systems synthetic to the main thrust (R and P fractures). These faults are marked by cataclasites with a shaly matrix that shows a scaly foliation defined by chlorite and pumpellyite, which also constrain the depth of faulting (8–10 km, T = 200–250 °C) within the seismogenic zone.

The central part of the fault also features the densest system of carbonate-filled veins. Veins occur in the broken formation matrix and fragments, in both cases parallel to the foliation. The veins are either folded, truncated, or pressure-solved along the cleavage. Cementation and hardening of shear surfaces of the fault core may have caused the distribution, as opposed to localization, of subsequent slip events. The fault core may have developed in basaltic rocks because of their inherently high permeability and propensity to transmit overpressure from deeper levels of the subduction zone.

Our analysis has shown that accretionary deformation is strongly controlled by injection of overpressured fluids occurring through systems of multiple dilatant fractures grossly parallel to the décollement zone. The crosscutting relationships between veining and foliation suggest that fluid injection is cyclic and, consequently, that large transient variations in permeability and cohesion may occur. The repeated injection of veins parallel to the fault zone may be explained by cyclic changes of the stress, or by difference in tensional strength parallel to and perpendicular to the foliation, both of which would require extremely high fluid pressure.

We interpret the features of the Rodeo Cove thrust zone as evidence of the seismic cycle and hypothesize a compressional stress field in the interseismic phase and an extensional stress field in the immediately postseismic phase.

Keywords: Franciscan Complex, accretionary prisms, seismogenic zone, hydrofracture, cataclasis, cyclic processes.

INTRODUCTION

Subduction fault zones produce the planet's largest earthquakes. We can remotely sense their behavior through refection seismology (Bangs et al., 2004), from earthquake seismology (Bilek and Lay, 1999), and geodetic information (Rogers and Dragert, 2003). Direct sampling of representative rock samples at the outcrop scale allows high-resolution investigation of subduction-related processes inferred from the above "remote sensing" techniques. Because deep drilling into subduction zones is not expected until near the end of this decade, exhumed outcrops of subduction thrusts provide valuable information about subduction zone seismogenesis.

Accretionary prisms grow by transfer of underthrust sediments and rocks from the downgoing plate to the overthrusting plate through the plate-boundary thrust (e.g., Moore and Sample, 1986; Sample and Fisher, 1986; Hashimoto and Kimura, 1999; Bangs et al., 2004). Thus, the plate-boundary thrust is incrementally and repeatedly preserved along the boundaries of each package that is transferred to the accretionary prism. By investigating thrust faults bounding rock packages accreted under the pressure-temperature (*P-T*) conditions of subduction zone earthquakes, we can examine processes associated with seismogenic deformation (e.g., Moore et al., 2006).

Direct examination of subduction thrusts can potentially address a number of questions regarding deformation and earthquakes in seismogenic zones. Since locking of the fault is required to allow strain accumulation, consequent earthquakes, and stress drops (~30 bars; Kanamori and Anderson, 1975), the fundamental question is what controls the onset of locking in the subduction thrust system? What types of incremental processes of lithification, phase transformations, or fluid-pressure changes lead to the locking and onset of earthquakes with depth along subduction thrusts?

Seismogenic slip occurs by increase of differential stress until it exceeds the yield strength of the rock (Scholz, 2002). The onset of unstable slip, or seismic behavior, in fault zones has been attributed to many factors, including changes in mineral phases with underthrusting in subduction zones (Vrolijk, 1990; Moore and Saffer, 2001), increases in fluid pressure or fault-valving (Sibson, 1990), the breakdown of cohesion (Muhuri et al., 2003), and compaction and consequent overpressuring (Sleep and Blanpied, 1992). Stick-slip models for earthquake generation have outlined the effect of mineral precipitation on earthquake potential of faults (e.g., Brace and Byerlee, 1966; Hill, 1977; Dieterich, 1978; Sibson, 1987, 1989, 1990, 1992; Scholz, 2002). A number of these mechanisms include changes in the time-dependent frictional behavior of the fault material with depth (Marone, 1998).

[†]E-mail: meneghini@dst.unipi.it.

GSA Bulletin; January/February 2007; v. 119; no. 1/2; p. 174–183; doi: 10.1130/B25807.1; 10 figures; 1 insert; Data Repository item 2007001.

In summary, there are both mineralogical and physical criteria to distinguish faults that may have formed by creep or accelerating slip (velocity-weakening versus velocity-strengthening behavior). Thus, although there is continuing debate in the structural geologic community about what structures really record an earthquake, short of pseudotachylyte (Cowan, 1999), the investigation of ancient thrust outcrops can focus on whether they developed any of the features that are inferred to cause the onset of seismic behavior. This evaluation requires attention to fault fabric, the development of mineral phases during faulting, evidence for solution and cementation in the fault, and evidence for overpressure and fluid flux through the fault.

Changes in subduction thrusts that cause seismogenic behavior will be most apparent with the comparison of a number of examples that have been deformed above, within, and below the occurrence interval of thrust earthquakes. We report here on the structural study of a thrust, the Rodeo Cove thrust, which bounds an accreted package of oceanic basalt and sedimentary rock. This fault occurs within an accreted terrane made up of thrust packages of oceanic rocks that are bounded by thrusts similar to the Rodeo Cove thrust. This thrust is a good example of a paleo-décollement that was active at *P-T* conditions typical of the upper seismogenic zone of subduction thrust earthquakes (see following).

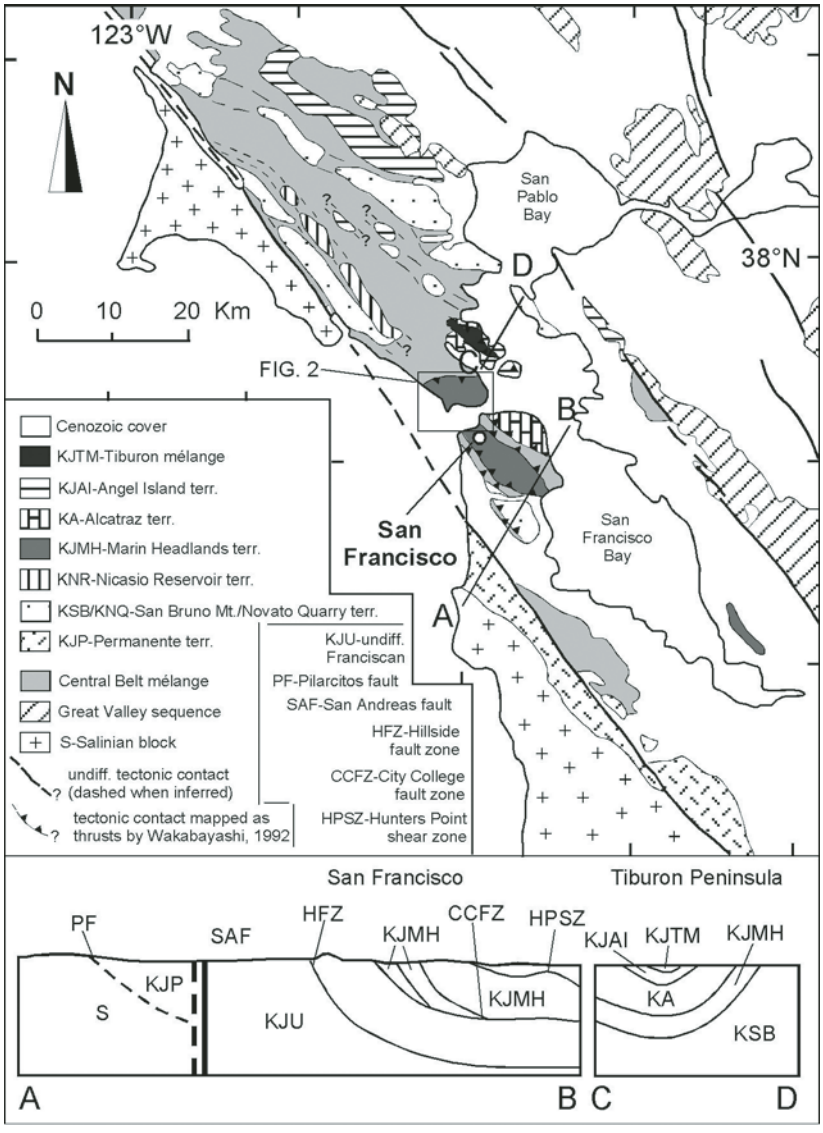

Figure 1. Franciscan Complex of the San Francisco Bay area. A–B and C–D cross sections are shown on bottom of figure. Map is based on Blake et al. (1984); Wahrhaftig (1984, 1989); and Wakabayashi (1992).

In order for an exhumed subduction thrust to preserve its emplacement history in the seismogenic zone, deformation must be isolated from previous and subsequent events: subsequent deformation must be mild, or at least clearly overprinting earlier deformation. Moreover, deformation may or may not be acquired during underthrusting of the oceanic package prior to emplacement in the seismogenic zone. This deformation must be separable from the faulting associated with emplacement. Fortunately, the synchrony of metamorphic climax and main deformation in the Rodeo Cove thrust suggests that this event represents the underplating of the terrane to the accretionary prism (see discussion of Van Gool and Cawood, 1994). Therefore, it is likely that each bounding thrust represents a once-active portion of the décollement or plate-boundary thrust. Later deformation is very weak and always clearly distinguished from the main deformation event.

At Rodeo Cove, an extraordinary exposure of the thrust, created by wave erosion, has allowed a detailed analysis, at the centimeter scale, of a structural profile approximately normal to the thrust dip (Fig. DR1[1]). Field study, accompanied by a careful microscopic to ultramicroscopic scale analysis, has focused on contrasts among hanging-wall, footwall, and shear zone deformational features.

GEOLOGIC SETTING OF THE RODEO COVE THRUST AND ASSOCIATED FRANCISCAN COMPLEX

The Franciscan Complex crops out in central California, on the eastern side of the San Andreas fault, and is associated with three geological subparallel domains (Sierra Nevada Batholith, Great Valley Sequence, Coast Range ophiolite), which are interpreted as different components of a subduction complex related to underthrusting of the Pacific plate under the western North American plate margin (Blake et al., 1984; Wakabayashi, 1992). The Franciscan Complex (Fig. 1) is interpreted as the accretionary wedge built by offscraping and underplating of numerous fault-bounded units, from ca. 150 Ma until the onset of a transform tectonic regime ca. 30 Ma (Wahrhaftig, 1989; Wakabayashi, 1992).

The Franciscan terranes' typical stratigraphic succession consists of ophiolitic sequences capped by deep-sea fan and trench deposits.

[1]GSA Data Repository item 2007001, Figure DR1, structural profile showing all of the major structural features, is available on the Web at http://www.geosociety.org/pubs/ft2007.htm. Requests may also be sent to editing@geosociety.org.

These sequences crop out as coherent units surrounded by highly disrupted units, mostly reduced to tectonic mélanges, defined by exotic blocks embedded in a sheared scaly matrix (Cloos, 1982; Blake et al., 1984; Wakabayashi, 1992; Jeanbourquin, 2000). Mélanges up to 1500 m thick mark the thrust zones bounding coherent units, and thinner stratally disrupted units, resulting from contemporaneous internal imbrication, have been interpreted as analogues of plate-boundary fault zones (Wakabayashi 1992, 1999); similar structures are documented in the Alaskan Kodiak Complex (e.g., Fisher and Byrne, 1987; Sample and Moore, 1987; Kusky et al., 1997) and in the Shimanto Complex of SW Japan (e.g., Kimura and Mukai, 1991; Hashimoto and Kimura, 1999).

Depending on the depth of accretion, the units have experienced a subduction-related metamorphism ranging from zeolite to eclogitic facies (Ernst, 1984).

The Bay Area of San Francisco (Blake et al., 2000) shows well-preserved products of subduction and accretion (Fig. 1) in the form of coherent units bounded by mélange units interpreted as analogues of thick plate-boundary zones (Wakabayashi, 1992). Except for some pervasive strong deformation near the San Andreas fault, the Franciscan Complex outcropping in the Bay Area is the least affected by Neogene deformation, providing the best field area to examine the Franciscan structural evolution (Wakabayashi, 1992). The Marin Headlands is one of the best known Franciscan terranes from a stratigraphic and structural perspective.

The Marin Headlands Terrane

The thrust that we studied is part of the Marin Headlands terrane, outcropping just north of Golden Gate Bridge (Figs. 1 and 2). The terrane is composed of a complex array of SSE-dipping, ENE-WSW–striking coherent tectonic slices, 300–500 m in thickness, characterized by a low-grade metamorphism of prehnite-pumpellyite facies (Wahrhaftig, 1984; Wakabayashi, 1999). Although the main structural trend for Franciscan terranes strikes NW and dips NE (Fig. 1), the Marin Headlands terrane strata and internal shear zones dip S to SSE, due to a 90° to 130° clockwise rotation of the Marin Headlands block (Blake et al., 1984; Curry et al., 1984; Wakabayashi, 1999).

Despite pervasive internal imbrication, the stratigraphic succession can be reconstructed for the Marin Headlands terrane; it consists of coherent pillow lava bodies, thinly bedded Jurassic to Cretaceous radiolarian cherts, and Albian to Cenomanian turbiditic sequences (Wahrhaftig, 1984). Biostratigraphy indicates

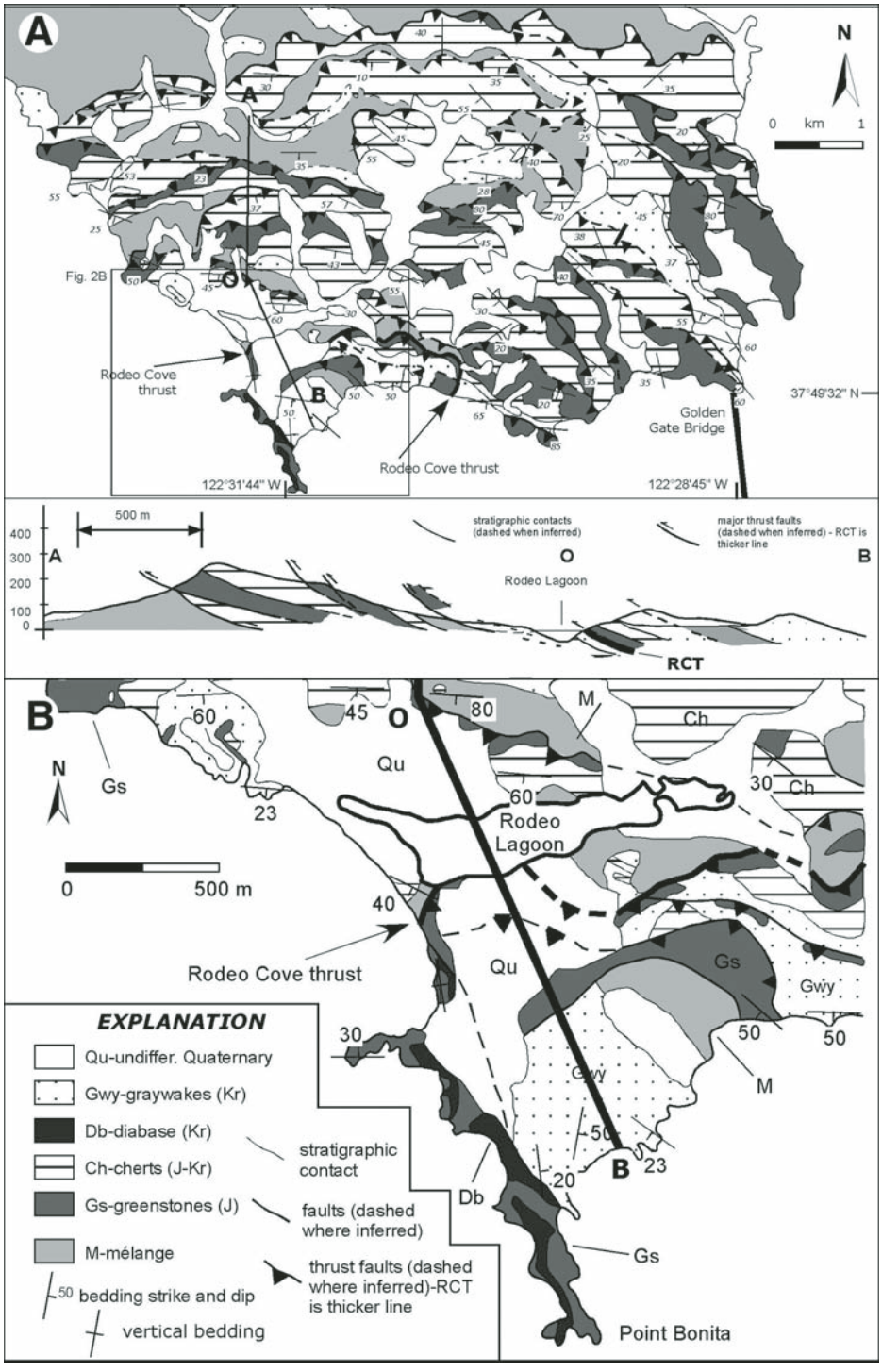

Figure 2. (A) Geologic map of the Marin Headlands peninsula, north of San Francisco, after Blake et al. (2000) (location in Fig. 1). The cross section, constructed after field work, shows thin sandstone and chert units overthrust by basalts through the Rodeo Cove thrust (RCT). (B) Close-up view of Rodeo Lagoon geology.

Figure 3. Line drawing from pictures of the Rodeo Cove thrust.

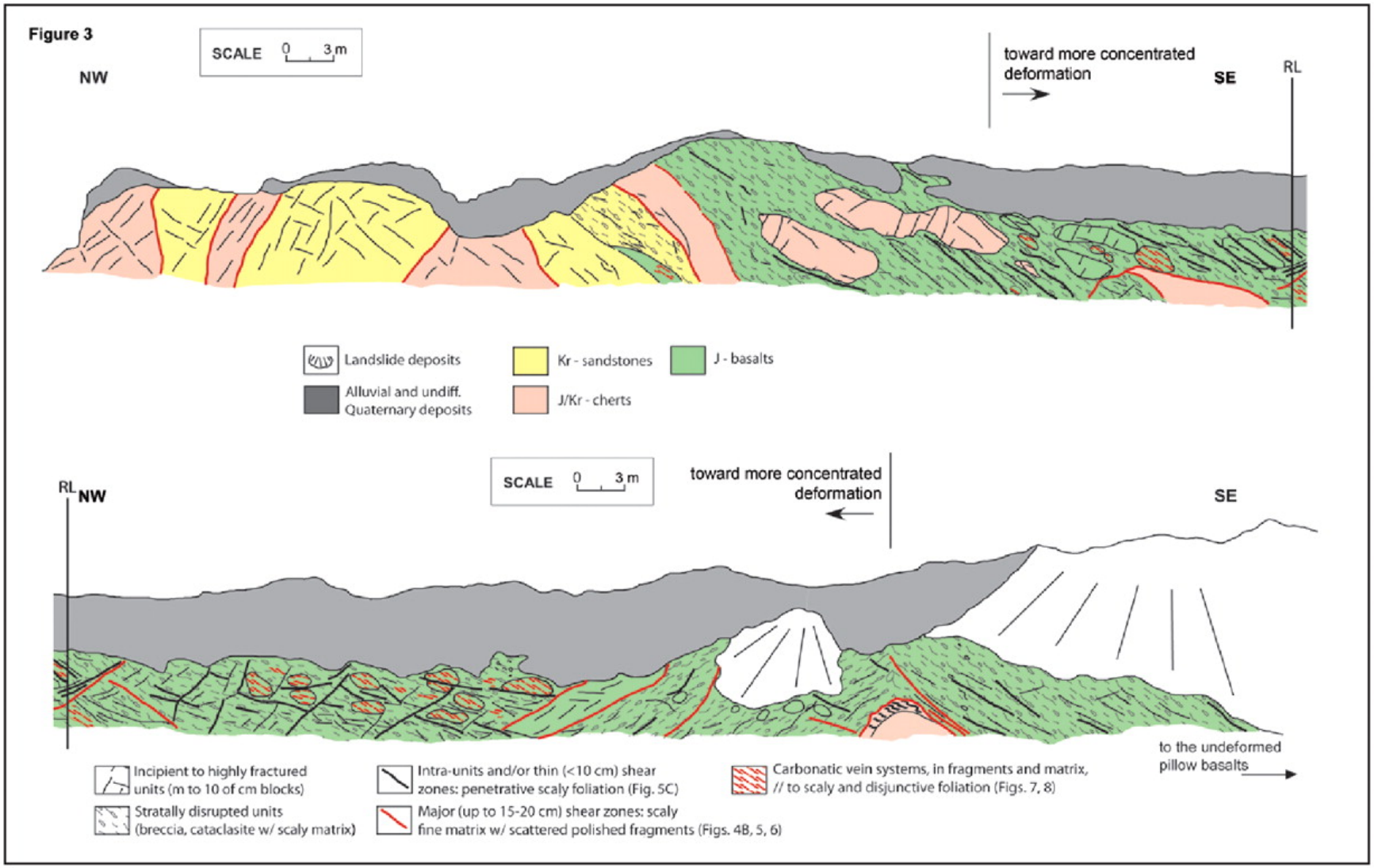

Figure 3. Line drawing from pictures of the Rodeo Cove thrust. RL—reference line for section truncation in figure.

Meneghini F , and Moore J C Geological Society of America Bulletin 2007;119:174-183

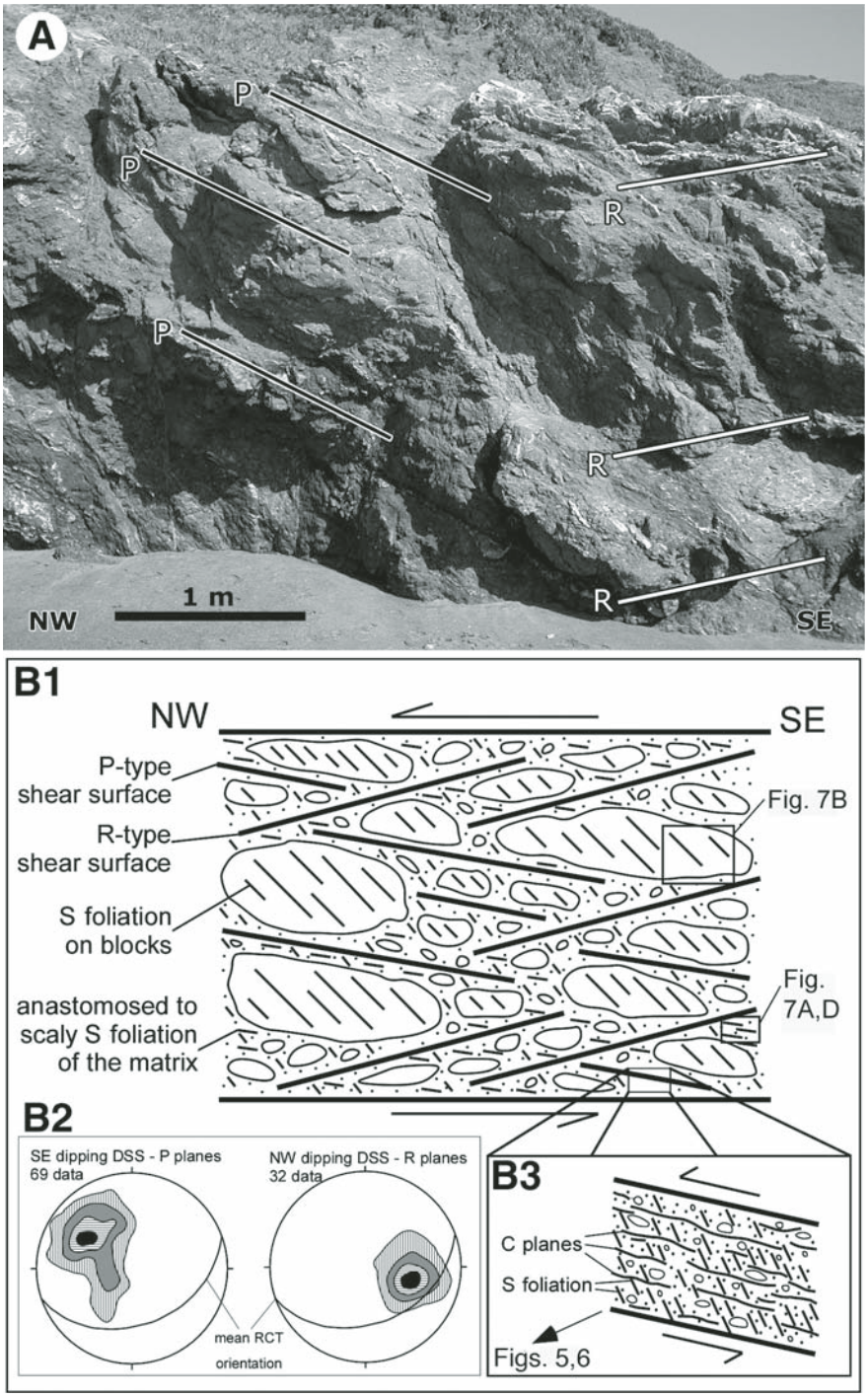

Figure 4. Typical features of fault broken formation. (A) P and R Riedel arrangement of discrete shear surfaces disrupting basalts of the fault core. Main shear zone is indicated with arrows. (B) Schematic section of typical geometrical arrangement of P and R discrete shear surfaces with respect to main shear zone. Although foliations are anastomosing surfaces, they are schematically represented as thin straight lines. Along S foliations, in (B1) and (B3), thin and thick veins also occur (see Fig. 8). (B1) S foliation on basaltic blocks grossly parallels the scaly foliation of the matrix. Straight lines also represent pressure-solution surfaces. (B2) Lower-hemisphere poles projections of the two main systems of discrete shear surfaces. The great circle represents the mean, map-scale orientation of the Rodeo Cove thrust (RCT). (B3) Schematic close-up of discrete shear surface showing scale invariant cataclastic aspect made up by clasts wrapped by a very fine matrix, showing scaly fabric and S-C structures. S foliation in P planes makes a very low angle with S foliation outside the discrete shear surfaces. DSS—discrete shear surface.

that this stratigraphic succession is repeated many times by thrusts faults (Murchey, 1984).

THE RODEO COVE THRUST ZONE

The Rodeo Cove thrust outcrops at Rodeo Beach and has a structural thickness of ~200 m (Figs. 2 and 3[2]). The outcrop lies at the southern end of the Rodeo Lagoon and, with the exception of a landslide in the southeastern part of the outcrop, is exceptionally well exposed because the coastline runs at a high angle to the fault strike, making it possible to conduct detailed mapping and analysis of the thrust zone. The thrust strike is approximately ENE-WSW, with a N-NW vergence, consistent with the mean attitude of the mélange zone bounding the entire terrane. The Rodeo Cove thrust imbricates two tectonic slices belonging to the Marin Headlands terrane, juxtaposing pillow basalts over a chaotic chert-sandstones sequence (Figs. 2 and 3).

Despite a landslide, the eastern end of the thrust is defined by a gradual transition to undeformed pillow basalts of the hanging wall (Fig. 3), while on the west, the alluvial deposits of Rodeo Lagoon and Beach cover the western side of the thrust outcrop. Accordingly, the original thickness of the thrust might have been greater than what actually is preserved. It is not easy to establish the displacement along the shear zones, because of the disrupted nature of the lithologies and the lack of offset features in the basalts, and offset fragments cannot be correlated across the faults for distances of more than 1 m along any shear surface comprising the thrust zone. However, the basalt-chert-sandstone stratigraphic sequence, originally many hundreds of meters thick, was repeated along a low-angle fault. This implies a minimum of many hundreds of meters of total displacement for the entire fault zone.

Structural Zonation of the Rodeo Cove Thrust

Figures 3 and DR1 (see footnote 1) show the structural section measured normal to the thrust dip, which documents all the major structural features recognized at the outcrop. The thrust outcrop is dissected by a complex fracture network that created smaller units (Fig. 4A), characterized by different lithologies and deformation features. Moving from the footwall up structure, the first third of the outcrop is occupied by a dense alternation of internally coherent units of sandstone and chert. This sandstone and

[2]Figures 3, 5, 6, 7, and 8 are on a separate sheet accompanying this issue. They can also be viewed online at http://www.dx.doi.org/10.1130/B25807.S1.

Figures 5-8.

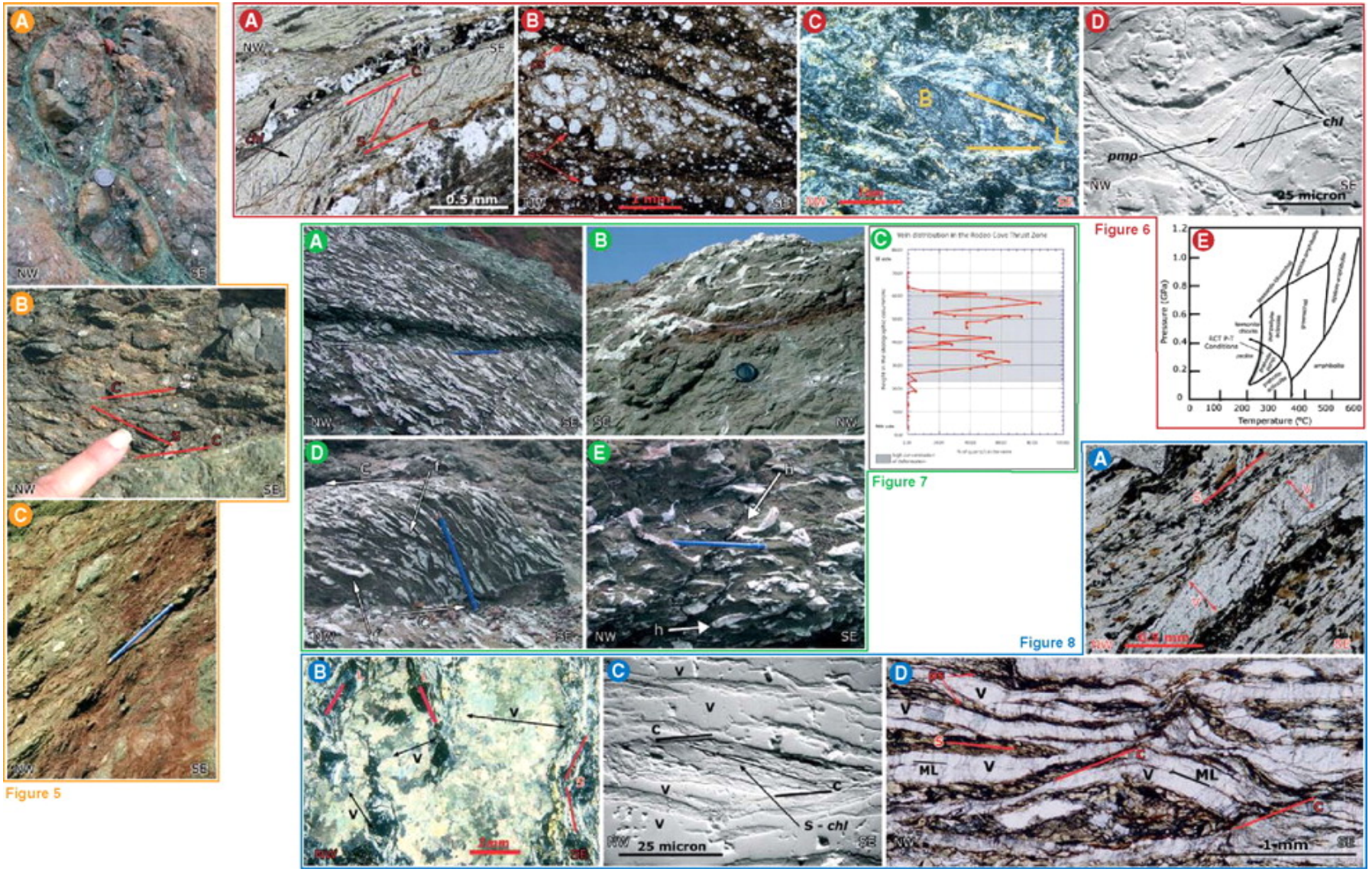

Meneghini F , and Moore J C Geological Society of America Bulletin 2007;119:174-183

chert unit is structurally overlain by a highly disrupted basaltic unit that grades to less-deformed basalts of the hanging wall. The fracture network includes brittle shear zones associated with the main thrust, suggesting that the thrust developed through localization of deformation into discrete surfaces (see next section). These faults are arranged in two systems intersecting at angles of 15°–25° (Fig. 4). Kinematic and structural analyses at the mesoscale (i.e., S-C brittle structures, asymmetry, and sense of elongation of rigid clasts, striae) reveal a top-to-the-NW sense of shear for both shear planes. These data, together with thrust vergence and mean map-scale attitude, suggest that the shear surfaces are R and P planes of the Riedel shear model (e.g., Riedel, 1929; Tchalenko, 1968; Cowan and Brandon, 1994). Following the model, we refer to the NW-dipping planes as the R shear planes, and to the SE-dipping surfaces as the P shear planes (Fig. 4).

According to observations in upper crustal brittle faults (Chester and Logan, 1987; Chester et al., 1993; Caine et al., 1996; Chester and Chester, 1998; Caine and Forster, 1999), the localization of deformation allows the Rodeo Cove thrust internal structure to be described using the damage zone–fault core model (Caine et al., 1996; Caine and Forster, 1999). The fault core is defined as the interval that displays the highest concentration of deformation-related structures (e.g., fractures, minor shear zones, brecciation, mineral veins, etc.) and that accommodates most of the displacement. The damage zones are the peripheral intervals, grading to the undeformed protolith, that show less penetrative deformation. These fault zone components can be variably developed in a shear zone, giving rise to different architectures (Caine and Forster, 1999). The central part of the Rodeo Cove thrust outcrop is characterized by 30–40 m of a highly disrupted basaltic unit. The unit is locally a broken formation generated by progressive stratal disruption, penetrative fracturing, and cataclasis (Figs. 3, 4, and 5). The basalts are dissected by the densest observed system of discrete slip surfaces (next section). Here decimeter- to meter-sized blocks show a variably spaced foliation, and the highest density of vein development has been identified (Fig. 3; Fig. DR1 [see footnote 1]). Similar vein distributions have been observed in cores of mature fault components of the San Andreas fault system (Chester et al., 1993), although the Rodeo Cove thrust displays a much higher vein concentration than those observed by Chester and co-workers. This central zone of concentrated deformation grades toward the eastern and western lateral sides of the outcrop, distinguished by a decrease in mesoscopic deformation, fractures, and vein density (Figs. 3 and DR1). These damage zones above and below the central core can be traced continuously over a structural thickness of 20–30 m before the outcrop is lost to alluvium on the west and to a landslide on the east. The damage zones are comprised of mappable chert, sandstone, and basalts units that feature brecciation, fracture, and joint sets and web structures in the sandstones (complex arrays of shear bands, see Byrne, 1983), juxtaposed by the network of discrete slip surfaces.

Discrete Slip Surfaces

The deformation and the displacement in the Rodeo Cove thrust occurred by development at all scales of discrete slip surfaces, which are arranged as R and P Riedel shear planes and range in thickness from the millimeter to the decimeter scale (Figs. 4 and 5). They cut all lithologies and increase in density toward the center of the outcrop, or fault core, where clusters of concentrated deformation occur.

The discrete slip surfaces are sites of concentrated deformation isolating less-deformed competent blocks that usually preserve their primary textures (Fig. 5A). The discrete slip surfaces are marked by cataclasites composed of millimeter- to decimeter-sized elongate fragments enclosed in a greenish or reddish fine mixture of very fine siltstone and shale (Figs. 5 and 6). The fragments show lenticular shapes and various dimensions (Figs. 5A, 6B, and 6C), and display pervasive brecciation, with variably spaced networks of intragranular and transgranular fractures. The matrix shows a penetrative foliation, the aspect and intensity of which are closely dependent on clast size and frequency. In general, the foliation is scaly (Figs. 5C and 6A), i.e., a system of anastomosing polished or striated shear surfaces pervasive on a scale of millimeters (Lundberg and Moore, 1986; Labaume et al., 1997a; Vannucchi et al., 2003). The scaly foliation is associated with other less-abundant shear fabrics, such as polished and striated fragment surfaces and brittle S-C structures (Figs. 5B and 6). The C-type plane mean attitude approximates a plane striking N20°E–N35°E, which is consistent with the average strike of both R and P planes. The S-type foliation is approximately parallel to a spaced cleavage observed in the competent, basalt blocks (Fig. 4B). The shear sense of all these structures is always top-to-NW, which is consistent with that inferred for the main thrust.

Microscopically, the discrete slip surfaces show well-preserved to strongly weathered competent cores of variable size, dispersed in a finer matrix (Figs. 6B and 6C). Fabric is mainly cataclastic, and is characterized by extreme grain size reduction, large range in grain size, sharp and angular fragment boundaries, and fine scaly matrix surrounding competent clasts (Figs. 6B and 6C). The fine foliated matrix of the slip surfaces is composed of a mixture of chlorite and clay minerals (Fig. 6; see also Fig. 8). These minerals have a strong concentration in the discrete shear surfaces compared to the fragments, very-fine grain size, and intergrowth, which all suggest that they are syntectonic and preferentially oriented along cleavage lamellae arranged in an anastomosing web around the competent fragments (Fig. 6A–C). Thin layers of hydroxides and opaque residual minerals bound the fragments and are concentrated along the edge of the clasts that frequently show sutured contacts; apparently, pressure solution accompanied cataclasis (Figs. 6B and 8D). Fragmentation and reorientation of clasts (B of Fig. 6C) and pre-existing minerals occur parallel to the scaly foliation.

Chlorite recrystallization records the opening and development of fractures through shear, as demonstrated by chlorite grown in S-C brittle structures (Figs. 6A, 6D, and 8C). Acicular pumpellyite is often intimately associated with chlorite in these structures (Fig. 6D), demonstrating that this mineral phase formed during thrust deformation, during subduction, and not during oceanic hydrothermal alteration. More importantly, the association of pumpellyite and chlorite in the cleavage lamellae (Fig. 6D), and the occurrence of laumontite across the terrane (Schlocker, 1974; Swanson and Schiffman, 1979), constrain the *P-T* conditions of deformation to ~2.5 kbar and 200–300 °C (Fig. 6E).

Mineralization and Veins Distribution

Veins occur in the damage zones and increase in frequency toward the center of the outcrop, where they locally make up ~80% of the outcrop area (Figs. 3 and 7; Fig. DR1 [see footnote 1]). Thus, the fluid circulation and related fluid-rock interactions were localized where the discrete shear surface network is densest.

The veins are found both in competent blocks and in the fine scaly matrix of the discrete slip surfaces (Fig. 7, see also Fig. 4). Two vein textures are generally recognizable, depending primarily on vein thickness. The two types of veins have grossly the same geometries, are calcite and rarely quartz filled, but show different distributions. The thickest veins are generally 1 cm thick and occur generally in the sandstone and basalt blocks (Fig. 7). They show variable thickness along their strike, with sharp, pinched terminations and boudinage. Lateral continuity ranges from <5 cm up to ~50 cm. The thinner veins never reach 1 cm in thickness, and are generally <5–6 mm thick. They develop along

the discrete slip surfaces, or in association with finer lithologies, although, locally, they can be found in the highly disrupted basalt blocks. The thin veins show more continuous lateral extension compared to the thick set and are generally 50–60 cm long and occur as repeated sets of parallel veins (Fig. 7A).

Both types of veins show sharp boundaries and "clear" vein fillings, with a very low percentage of wall-rock particles, and record extensional strain (Fig. 8A). Locally, some calcite crystals show type I and II twins (from Burkhard, 1993), suggesting twinning at 150–300 °C. The thickest veins always display mosaic, blocky textures defined by irregular arrangement of clear anhedral calcite crystals, locally intergrown with less-abundant quartz crystals (Fig. 8B). A well-developed fibrous texture is locally visible in some of the thinner veins, where antitaxial straight, calcite fibers (Fig. 8D) occur together with scattered, irregular, dark median lines.

Despite the slightly different distribution, thick and thin veins show similar arrangements with respect to foliation and slip planes, lying parallel to both the anastomosing spaced foliation of the competent blocks and the S-planes in the scaly foliation of the matrix (Figs. 7 and 8). Discontinuous films of opaque, residual minerals also parallel S-planes and veins (ps in Fig. 8D). This observation, together with frequent stylolite occurrence in the calcite filling, supports the interpretation of pressure solution.

Crosscutting relationships between veins and foliation have been observed from meso- to microscale (Figs. 7 and 8). For example, veins, as well as S-planes and pressure-solution seams, are often rotated and truncated by the C planes of scaly foliation marked by fine-grained chlorite and opaque mineral seams (Figs. 7D, 8C, and 8D). Vein deformation also occurs close to isoclinal folds with acute hinges and tight limbs (Figs. 7D, 7E, and 8B). The limbs lie along two crosscutting fracture planes, paralleling the discontinuous chlorite layers that define the anastomosing foliation (Fig. 8B). Limbs are frequently thinned and stretched along the planes, so that most of these veins appear as isolated fragments (Fig. 7E).

DISCUSSION AND INTERPRETATION

Structural Development of the Rodeo Cove Thrust

The Rodeo Cove thrust imbricates two tectonic slices belonging to the Marin Headlands terrane. The thrust is parallel to the unit-bounding shear zones that make up the entire terrane, and shows the same vergence and attitude, and same metamorphic conditions. The Rodeo Cove thrust does not deform or cut across other faults, so it can be considered as part of this thrust imbrication. Particularly, the entire Marin Headlands terrane can be interpreted as a series of underplated duplexes forming at the same *P-T* conditions.

The depth and temperature range of accretion inferred from the preserved metamorphic minerals along the Rodeo Cove thrust falls within the typical depth of seismogenic zones of subduction thrusts, suggesting that the thrust acted at seismogenic depth or immediately below the aseismic to seismic transition. In fact, this transition along subduction margins has been estimated to occur at around 4 km depth, from relocation of recorded earthquakes (Bilek and Lay 1999), and along the ~125° isotherm, by using a thermal proxy (Hyndman et al., 1997; Oleskevich et al., 1999).

The Rodeo Cove thrust crops out as a variably deformed, copiously veined, 200-m-thick fault zone in which strain is accommodated primarily by discrete slip surfaces, which occur on millimeter to meter scales and are typical of active accretionary thrusts (e.g., Lundberg and Moore, 1986; Labaume et al., 1997a) and shallow faults and gouges (Chester et al., 1993; Caine et al., 1996; Chester and Chester, 1998, Labaume and Moretti, 2001).

Upper crust fault zones show complex architectures made by variably distributed components, such as a fault core and a damage zone (Caine et al., 1996; Caine and Forster, 1999). The evolution of fluid flow in these faults can vary greatly depending on the particular distribution of fault zone components (Caine and Forster, 1999). Following this model, and taking into account the lack of part of the exposure and of clear constraints on displacement versus deformation, the Rodeo Cove thrust zone can be described as part of a thick distributed deformation zone (DDZ of Caine et al., 1996; and Caine and Forster; 1999). As widely described, localization of deformation occurs from meso- to microscale, and throughout the entire exposure, by a variably distributed complex network of discrete shear surfaces. Concentration of deformation characterizes the central part of the outcrop, where an increase in number and density of shear surfaces and a major degree of disruption are documented. This zone only involves basalts, suggesting a possible lithologic control on localization of deformation during thrust activity. The discrete shear surfaces arrangement can also be compared to the distributed-localized shear (DLS) deformation pattern defined by Jeanbourquin (2000) for the Franciscan mélange outcropping at Pacifica, south of San Francisco. The DLS is described as a complex anastomosing array of narrow shear surfaces concentrated in bands.

The main features observed in the discrete slip surfaces, i.e., the extreme grain size reduction, grain alignment, and the scaly foliation, are interpreted as the result of shear-related compactional strain. The fabric observed in the slip surfaces suggests that cataclastic flow, as defined by Passchier and Trouw (1996), was the main deformation mechanism. Shear-related compaction, cataclasis, and disaggregation decrease the lithification state of some zones, allowing intragranular particulate flow to accompany cataclastic flow. The subsequent reorientation of grain fragments parallel to the S foliation caused porosity to collapse in the slip surfaces with respect to the host rocks. Parallel to S foliation are seams of opaque minerals, which are interpreted as the result of pressure solution around the competent clasts. These mechanisms contributed to the sealing of the fractures and are interpreted to have lowered both porosity and permeability.

Vein Development and State of Stress in the Rodeo Cove Thrust Fault

The high concentration of veins in the Rodeo Cove thrust indicates flow of fluid along the thrust zone. The veins represent Mode I fractures, recording episodes of pore pressure buildup (e.g., crack-seal of Ramsay, 1980). Moreover, the meso- and microscale analyses of vein features indicate that vein growth was structurally controlled by fractures, and the hydrofractures opened along the pre-existing, relatively weak surfaces that define both scaly fabric and disjunctive foliation. The tabular geometry of veins and their macroscopic and microscopic regularity seem to confirm this hypothesis. The straight, sharp vein boundaries also suggest structurally controlled vein growth, although this feature can be partly correlated to the high competence of the host basalt. Higher competency of the basalts not only implies that it is stronger than the sediments but that it is also more brittle and, consequently, can facilitate extensional strain localization. This observation may also explain the concentration of veining in basaltic lithotypes.

Alternatively, the veins could have formed at a steeper angle, in the extensional direction of a simple shear couple, and then subsequently undergone rotation into the fault surface. The pressure-solution surfaces would have been forming simultaneously in the plane of maximum flattening of the shear couple. Although we do see folded veins, we do not see examples of progressive rotation of veins nor development of veins with large angular differences from the

foliation and shear surfaces. Thus, we do not favor this interpretation.

Crosscutting relationships between the thick and thin types of veins and their similar arrangement with respect to the structural elements suggest that they probably formed simultaneously. Thus, they are then referable to the same deformation phase. Lithification-dependent dilatancy may also justify the different textures and distributions of the observed veins. Thick veins develop into the preserved basalt blocks because they are more brittle than the matrix, so they dilate more easily. In fact they develop an intense disjunctive cleavage. On the contrary, the matrix is dominated by sets of millimeter-thick veins, apparently because dilatancy is minimized in this relatively low-strength material. Therefore, in the matrix, the episodes of high pore pressure caused the opening of smaller fractures that were easily filled by fluids. This is supported by the fibrous texture, which characterizes only the thinner veins; the mosaic texture of the thick veins may indicate that growth rate was unable to keep pace with fracture opening.

The occurrence of dilatant structures (hydrofractures and veins) along compactional structures (scaly foliation surfaces) has been observed also at shallower levels in modern accretionary margins (Labaume et al., 1997b) and is interpreted as the result of cyclic variations of the stress controlled by variations of pore pressure. Crosscutting relationships among foliation development, pressure solution, and vein formation in the Rodeo Cove thrust (Fig. 8B–8D) support the above-cited model, suggesting that a sequence of fracturing, vein formation, and development of anastomosing to scaly foliation through shear and solution repeated cyclically. In each cycle, scaly foliation formation occurred during low-fluid-pressure episodes, as a result of shear-related compactional strain. Similarly, the pressure-solution surfaces formed perpendicular to the maximum principal stress (Fletcher and Pollard, 1981), implying a local stress field such as that indicated in the upper part of Figure 9. Conversely, high-fluid-pressure episodes and hydraulic opening of pre-existing fractures imply extension, perpendicular to the minimum principal stress, with no large component of shear (Fig. 9A). Then, the parallelism of the carbonate veins and the pressure-solution surfaces (Fig. 8D) suggest that the minimum and maximum principal stresses may have switched ~90 degrees between the periods of formation of these features. Alternatively, a significant difference in tensional strength parallel to and perpendicular to the foliation may explain vein formation parallel to the S planes and the pressure-solution seams, without requiring rotation of the principal stresses (Fig. 9B). In order for a hydrofracture to occur, the fluid pressure must overcome the tensile strength of the material (Secor, 1965). If a significant difference exists in tensile strength parallel and perpendicular to the foliation, an increase in fluid pressure may result in a shifting of the Mohr circle past the origin of the Mohr diagram, so that both σ_1 and σ_3 become tensile stresses. If the pressure rises such that σ_1 becomes tangent to the failure envelope parallel to foliation, but σ_3 has not yet reached the failure envelope perpendicular to foliation, then an extension fracture parallel to the foliation and perpendicular to σ_1 can occur. This requires the differential stress to be less than the difference in tensile strength parallel to and perpendicular to the foliation. Both of these interpretations require cyclical episodes of high fluid pressure.

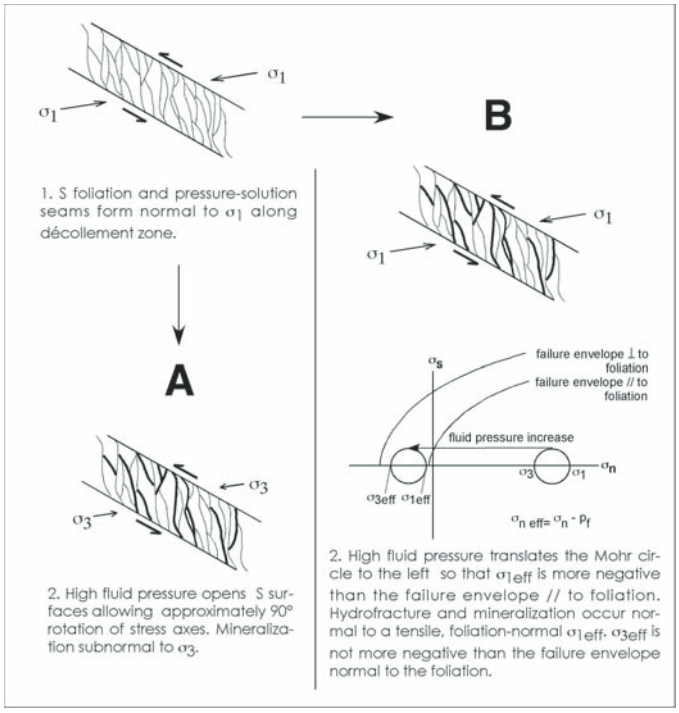

Figure 9. Possible states of stress responsible for the observed parallelism of veins and foliation and pressure-solution fabric. Stages 1 and 2 in both schemes refer to the same stages in Figure 10. (A) The principal stress axes switch when stress is released at failure. Veins form immediately postseismic leading to healing of the fault zone and stress reaccumulation. (B) The parallelism of veins and foliation and pressure-solution fabric can also be explained with a fixed stress orientation and a significant difference in tensional strength parallel to and perpendicular to the foliation.

Fault Evolution and the Seismic Cycle

Although the only clear, universally accepted fossil evidence of seismic slip are pseudotachylytes (Cowan, 1999), we have known since the 1970s the importance of fluid migration and mineralization in faults and fractures in triggering small earthquakes and promoting a stick-slip behavior of faults (Hill, 1977; Sibson, 1987, 1989, 1990, 1992). Starting from the inferred Rodeo Cove thrust evolution, and considering a fault-valve behavior of the thrust (e.g., Sibson, 1990), we can tentatively correlate the above-described deformation and hydrogeological cycling to the seismic cycle.

We suggest the following sequence of fabric formation (Fig. 10). (1) During compaction, in interseismic intervals, the shear zones experience high shear stress and S foliation and pressure-solution fabrics form almost perpendicular to high effective maximum principal stress. The fault behaves as an impermeable seal (Sibson, 1990, 1992). (2) Failure (possibly seismic?), stress relaxation, and high fluid pressure allow fault zones to dilate along S surfaces and pressure-solution folia. The thrust forms a highly permeable channel for fluids that flow until the hydraulic gradient reverts to hydrostatic (Sibson, 1990, 1992). (3) The pressure drop accompanying discharge causes mineralization, and relatively rapid precipitation of carbonate occurs (Fyfe et al., 1978). (4) Further mineral precipitation and lowered pore pressure would

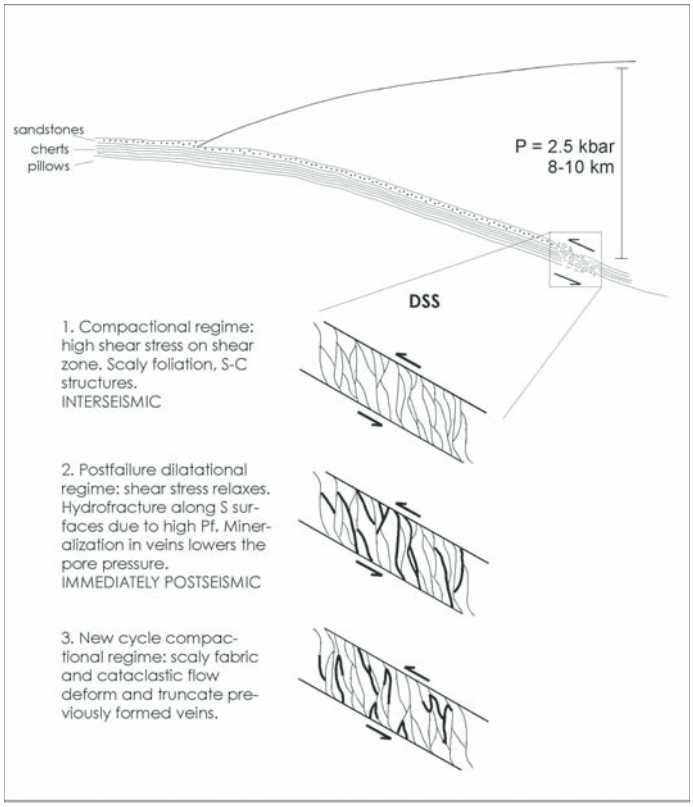

Figure 10. Conceptual model of deformation-related fluid circulation in the Rodeo Cove thrust (RCT), with possible relation to seismic cycle. Not to scale. (Stage 1) During compactional regime in interseismic intervals, the shear zones experience high shear stress and S foliation, and pressure-solution fabric form almost perpendicular to high effective maximum principal stress. (Stage 2) After (seismic?) failure, stress relaxation and high fluid pressure allow fault zones to dilate along S surfaces and pressure-solution foliation. Precipitation of carbonate occurs as pCO_2 is lowered and fluids exit through fracture permeability (Fyfe et al., 1978). (Stage 3) Return to interseismic compactional regime. DSS—discrete shear surface.

increase cohesion and effective stress, respectively, allowing the fault to strengthen (e.g., Sibson, 1990; Scholz, 2002) and stress to re-accumulate. The common occurrence of cataclasis and slickenlines may have developed during the relatively rapid seismic failure, but could also have occurred during interseismic periods along surfaces subject to shear failure.

Nonlocalized Slip and the Basaltic Composition Fault Core

The Rodeo Cove thrust shows several principal sliding surfaces (Figs. 3 and 4) rather than a narrow, well-defined fault core (e.g., Chester et al., 1993). We believe that this distributed deformation is due to the sealing of discrete slip surfaces with calcite and quartz veins, causing fault hardening and migration of slip elsewhere. Accordingly, only a limited number of slip surfaces were active during any seismic cycle, and the current volume of vein fillings was cumulative. Moreover, the significant slip expected from any large subduction zone earthquake could be distributed over a number of shear surfaces. Such distributed deformation has been reported from sedimentary mélanges interpreted as décollements (Fisher and Byrne, 1987) and attributed to hardening by dewatering (Moore and Byrne, 1987). Also, distributed deformation in a broad fault zone in granitic rocks is attributed to healing of fault surfaces by mineral precipitation and solidification of pseudotachylytes (Di Toro and Pennacchioni, 2005).

Why does the fault core occur in basaltic rocks? The sandstones and chert of the flanking damage zone is of similar or lower strength than the basalts (Byerlee, 1978; Morrow and Lockner, 2001). The concentration of veins in the basalt rather than the associated sandstones and cherts suggests that fluid flow concentrated in the basaltic fault core, presumably due to relatively higher permeability. The compactive deformation and diagenetic transitions in the sandstones and cherts would have reduced their permeability, and perhaps prevented migration of fluids away from the basaltic fault core. Studies of oceanic crust have suggested that the upper several hundred meters of pillow lavas can be a zone of higher permeability than the overlying sediments (Fisher, 2005). In this scenario, the downdip extension of the upper oceanic basement would allow it to tap into sources of high fluid pressure that would be transmitted updip through the basaltic aquifer, which would favor failure in this lithology (Kimura and Ludden, 1995).

CONCLUSIONS

The Rodeo Cove thrust provides the only high-quality exposure of the classic basalt-chert-sandstone imbricates of the Marin Headlands. Synmetamorphic chlorite and pumpellyite indicate that this thrust was active at temperatures of ~200–250 °C, where seismogenic behavior typically occurs. Thus, the Rodeo Cove thrust, and by implication the imbricated basalt-chert-sandstone sequences of the Marin Headlands, is interpreted as a series of underplated duplexes in the seismogenic zone. The fault deformational history shows an alternation of brittle deformation, vein formation, and pressure solution. The central 30–40 m of the fault is massively, extensionally veined by carbonate, and to a lesser degree, quartz. The veins are oriented parallel to the mean pressure-solution foliation. Thus, directions of extension during veining and directions of shortening during pressure solution are parallel. This enigma can be explained by either: (1) large-scale switching of principal stresses between the intervals of veining and pressure solution, or (2) veins forming parallel to fabric anisotropy due to the principal foliation, under small differences in principal stress magnitude. In either case, very high fluid pressure is required. We interpret the veining as having occurred immediately postseismic as a result of fluid pressure (including pCO_2) drop and consequent carbonate precipitation, and the S-C structures and pressure solution as the result of slow interseismic deformation. The cataclastic fabrics may be interpreted as having formed during slow deformation (e.g., Cowan 1999) or during fault movement at seismic slip velocities, which we favor. The absence of a localized principal slip surface indicates that the Rodeo Cove thrust fault failed along a series of distributed shear surfaces. The healing and hardening of slip surfaces by mineral precipitation discouraged their subsequent use, and additional slip events were accommodated by different fault strands. The

location of the core of the Rodeo Cove thrust in a basaltic lithology may have been due to its ability to preferentially transmit high fluid pressures from depth, creating a zone of weakness.

ACKNOWLEDGMENTS

Associate Editor J. Fletcher, J.S. Caine, J.C. Lewis, and two anonymous reviewers are gratefully thanked for helpful and thorough reviews that greatly improved the text. We thank Ernie Rutter for suggesting an alternate interpretation to our original hydrofracture scheme. Sampling access to the outcrops in Marin Headlands was provided by the National Park Service with the cooperation and assistance of Tamara Williams and Will Elder. This work was supported by National Science Foundation (NSF) grant 443754-22242 and Italian government grant Ministero dell'Istruzione, dell'Università e della Ricerca Scientifica COFIN 2003.

REFERENCES CITED

Bangs, N., Shipley, T.H., Gulick, S.P.S., Moore, G.F., Kuromoto, S., and Nakamura, Y., 2004, Evolution of the Nankai Trough décollement from the trench into the seismogenic zone: Inferences from three-dimensional seismic reflection imaging: Geology, v. 32, p. 273–276, doi: 10.1130/G20211.2.

Bilek, S.L., and Lay, T., 1999, Rigidity variations with depth along interplate megathrust faults in subduction zones: Nature, v. 400, p. 443–446, doi: 10.1038/22739.

Blake, M.C., Jr., Howell, D.G., and Jayko, A.S., 1984, Tectonostratigraphic terranes of the San Francisco Bay Region, *in* Blake, M.C., Jr., ed., Franciscan Geology of Northern California: Pacific Section, Society of Economic Paleontologists and Mineralogists Field Trip Guidebook, v. 43, p. 5–22.

Blake, M.C., Jr., Graymer, R.W., and Jones D.L., 2000, Geologic map and map database of parts of Marin, San Francisco, Alameda, Contra Costa, and Sonoma Counties, California: U.S. Geological Survey Miscellaneous Field Studies Map, MF-2337, scale 1:75,000.

Brace, W.F., and Byerlee, J.D., 1966, Stick-slip as a mechanism for earthquakes: Science, v. 153, p. 990–992.

Burkhard, M., 1993, Calcite twins, their geometry, appearance, and significance as stress-strain markers and indicators of tectonic regime: A review: Journal of Structural Geology, v. 15, p. 351–368, doi: 10.1016/0191-8141(93)90132-T.

Byerlee, J., 1978, Friction in rocks: Basel, Pageoph, Birkhauser Verlag, v. 116, p. 615–626, doi: 10.1007/BF00876528.

Byrne, T., 1983, Web structure, possible evidence for tectonic consolidation and dewatering in mélange: Eos (Transactions, American Geophysical Union), v. 64, p. 833.

Caine, J.S., and Forster, C.B., 1999, Fault zone architecture and fluid flow: Insights from field data and numerical modelling, *in* Haneberg, W., et al., eds., Faults and sub-surface fluid flow in the shallow crust: American Geophysical Union Geophysical Monograph 113, p. 101–127.

Caine, J.S., Evans, J.P., and Forster, C.B., 1996, Fault zone architecture and permeability structure: Geology, v. 24, p. 1025–1028, doi: 10.1130/0091-7613(1996)024<1025:FZAAPS>2.3.CO;2.

Chester, F.M., and Chester, J.S., 1998, Ultracataclasite structure and friction processes of the Punchbowl fault, San Andreas system, California: Tectonophysics, v. 295, p. 199–221, doi: 10.1016/S0040-1951(98)00121-8.

Chester, F.M., and Logan, J.M., 1987, Composite planar fabric of gouge from the Punchbowl fault, California: Journal of Structural Geology, v. 9, p. 621–634, doi: 10.1016/0191-8141(87)90147-7.

Chester, F.M., Evans, J.P., and Biegel, R.L., 1993, Internal structure and weakening mechanisms of the San Andreas fault: Journal of Geophysical Research, v. 95, p. 771–786.

Cloos, M., 1982, Flow mélanges: Numerical modeling and geologic constraints on their origin in the Franciscan subduction complex, California: Geological Society of America Bulletin, v. 93, p. 330–345, doi: 10.1130/0016-7606(1982)93<330:FMNMAG>2.0.CO;2.

Cowan, D.S., 1999, Do faults preserve a record of seismic slip? A field geologist's opinion: Journal of Structural Geology, v. 21, p. 995–1001, doi: 10.1016/S0191-8141(99)00046-2.

Cowan, D.S., and Brandon, M.T., 1994, A symmetry-based method for kinematic analysis of large-slip brittle fault zones: American Journal of Science, v. 294, p. 257–306.

Curry, F.B., Cox, A., and Engebretson, D.C., 1984, Paleomagnetism of Franciscan rocks in the Marin Headlands, *in* Blake, M.C., Jr., ed., Franciscan Geology of Northern California: Pacific Section, Society of Economic Palaeontologists and Mineralogists Field Trip Guidebook, v. 43, p. 89–98.

Dieterich, J.H., 1978, Time-dependent friction and the mechanics of stick-slip: Pure and Applied Geophysics, v. 116, p. 790–806, doi: 10.1007/BF00876539.

Di Toro, G., and Pennacchioni, G., 2005, Fault plane processes and mesoscopic structure of a strong-type seismogenic fault in tonalities (Adamello batholith, Southern Alps): Tectonophysics, v. 402, p. 55–80, doi: 10.1016/j.tecto.2004.12.036.

Ernst, W.G., 1984, California blueschists, subduction, and the significance of tectonostratigraphic terranes: Geology, v. 12, p. 436–440, doi: 10.1130/0091-7613(1984)12<436:CBSATS>2.0.CO;2.

Fisher, A.T., 2005, Marine hydrogeology: Future prospects for major advances: Hydrological Journal, v. 13, p. 69–97, doi: 10.1007/s10040–004–0400-y.

Fisher, D., and Byrne, T., 1987, Structural evolution of underthrusted sediments, Kodiak Islands, Alaska: Tectonics, v. 6, p. 775–794.

Fletcher, R.C., and Pollard, D.D., 1981, Anti-crack model for pressure solution surfaces: Geology, v. 9, p. 419–424, doi: 10.1130/0091-7613(1981)9<419:AMFPSS>2.0.CO;2.

Fyfe, W.S., Price, N.J., and Thompson, A.B., 1978, Fluids in the Earth's crust; their significance in metamorphic, tectonic and chemical transport processes: Amsterdam, Netherlands, Elsevier Science Publishing Co., 383 p.

Hashimoto, Y., and Kimura, G., 1999, Underplating process from mélange formation to duplexing: Example from the Cretaceous Shimanto belt, Kii Peninsula, southwest Japan: Tectonics, v. 18, p. 92–107, doi: 10.1029/1998TC900014.

Hill, D.P., 1977, A model for earthquake swarms: Journal of Geophysical Research, v. 82, p. 347–352.

Hyndman, R.D., Yamano, M., and Oleskevich, D.A., 1997, Seismogenic zone of subduction thrust faults: The Island Arc, v. 6, p. 244–260, doi: 10.1111/j.1440-1738.1997.tb00175.x.

Jeanbourquin, P., 2000, Chronology of deformation of a Franciscan mélange near San Francisco (California, U.S.A.): Eclogae Geologicae Helvetiae, v. 93, p. 363–378.

Kanamori, H., and Anderson, D., 1975, Theoretical basis of some empirical relationships in seismology: Bulletin of the Seismological Society of America, v. 65, p. 1073–1095.

Kimura, G., and Ludden, J., 1995, Peeling oceanic crust in subduction zones: Geology, v. 23, p. 217–220, doi: 10.1130/0091-7613(1995)023<0217:POCISZ>2.3.CO;2.

Kimura, G., and Mukai, A., 1991, Underplated units in an accretionary complex; mélange of the Shimanto belt of eastern Shikoku: Southwest Japan: Tectonics, v. 10, p. 31–50.

Kusky, T.M., Bradley, D.C., Haeussler, P.J., and Karl, S., 1997, Controls on accretion of flysch and mélange belts at convergent margins: Evidence from the Chugach Bay thrust and Iceworm mélange, Chugach accretionary wedge, Alaska: Tectonics, v. 16, p. 855–878, doi: 10.1029/97TC02780.

Labaume, P., and Moretti, I., 2001, Diagenesis-dependence of cataclastic thrust fault zone sealing in sandstones. Example from the Bolivian Sub-Andean zone: Journal of Structural Geology, v. 23, p. 1659–1675, doi: 10.1016/S0191-8141(01)00024-4.

Labaume, P., Maltman, A., Bolton, A., Tessier, D., Ogawa, Y., and Takizawa, S., 1997a, Scaly fabrics in sheared clays from the décollement zone of the Barbados accretionary prism, *in* Shipley, T.H., et al., Proceedings of the Ocean Drilling Program, Scientific Results, Volume 156: College Station, Texas, Ocean Drilling Program, p. 59–77.

Labaume, P., Kastner, M., Trave, A., and Henry, P., 1997b, Carbonate veins from the décollement zone at the toe of the Northern Barbados accretionary prism: Microstructure, mineralogy, geochemistry, and relations with prism structure and fluid regime, *in* Shipley T.H., et al., Proceedings of the Ocean Drilling Program, Scientific Results, Volume 156: College Station, Texas, Ocean Drilling Program, p. 79–96.

Lundberg, N., and Moore, J.C., 1986, Macroscopic structural features in Deep Sea Drilling Project cores from forearc regions, *in* Moore, J.C., ed., Structural Fabric in Deep Sea Drilling Project Cores from Forearcs: Geological Society of America Memoir 166, p. 13–44.

Marone, C., 1998, Laboratory-derived friction laws and their application to seismic faulting: Annual Review of Earth and Planetary Sciences, v. 26, p. 643–696, doi: 10.1146/annurev.earth.26.1.643.

Moore, J.C., and Byrne, T., 1987, Thickening of fault zones: A mechanism of mélange formation in accreting sediments: Geology, v. 15, p. 1040–1043, doi: 10.1130/0091-7613(1987)15<1040:TOFZAM>2.0.CO;2.

Moore, J.C., and Saffer, D., 2001, The updip limit of the seismogenic zone beneath the accretionary prism of SW Japan: An effect of diagenetic to low-grade metamorphic processes and increasing effective stress: Geology, v. 29, p. 183–186, doi: 10.1130/0091-7613(2001)029<0183:ULOTSZ>2.0.CO;2.

Moore, J.C., and Sample, J., 1986, Mechanisms of accretion at sediment-dominated subduction zones: Consequences for the stratigraphic record and the accretionary prism hydrogeology: Memorie della Società Geologica Italiana, v. 31, p. 107–118.

Moore, J.C., Rowe, C., and Meneghini, F., 2006, How can accretionary prisms elucidate seismogenesis in subduction zones?, *in* Dixon, T., and Moore, J.C., eds., The Seismogenic Zone of Subduction Thrust Faults: New York, Columbia University Press (in press).

Morrow, C.A., and Lockner, D.A., 2001, Hayward fault rocks: Porosity, density, and strength measurements: U.S. Geological Survey Open-File Report 01–421, 28 p.

Muhuri, S.K., Dewers, T.A., Thurmann, E.S.J., and Reches, Z., 2003, Seismic fault strengthening and earthquake-slip instability: Friction or cohesion: Geology, v. 31, p. 881–884, doi: 10.1130/G19601.1.

Murchey, B., 1984, Biostratigraphy and lithostratigraphy of chert in the Franciscan Complex, Marin Headlands, California, *in* Blake, M.C., Jr., ed., Franciscan Geology of Northern California: Pacific Section, Society of Economic Palaeontologists and Mineralogists Field Trip Guidebook, v. 43, p. 51–70.

Oleskevich, D.A., Hyndman, R.D., and Wang, K., 1999, The updip and downdip limits to great subduction earthquakes: Thermal and structural models of Cascadia, south Alaska, SW Japan and Chile: Journal of Geophysical Research, v. 104, p. 14,965–14,991, doi: 10.1029/1999JB900060.

Passchier, C.W., and Trouw, R.A.J., 1996, Microtectonics: Berlin, Springer-Verlag, 289 p.

Peacock, S.M., 1993, The importance of blueschist→eclogite dehydration reactions in subducting oceanic crust: Geological Society of America Bulletin, v. 105, p. 684–694, doi: 10.1130/0016-7606(1993)105<0684:TIOBED>2.3.CO;2.

Ramsay, J.G., 1980, The crack-seal mechanism of rock deformation: Nature, v. 284, p. 135–139, doi: 10.1038/284135a0.

Riedel, W., 1929, Zur Mechanik geologischer Brucherscheinungen: Centralblatt fur Mineralogie, Geologische und Paleontologie, v. 1929B, p. 354–368.

Rogers, G., and Dragert, H., 2003, Episodic tremor and slip on the Cascadia subduction zone: The chatter of silent slip: Science, v. 300, p. 1942–1943, doi: 10.1126/science.1084783.

Sample, J.C., and Fisher, D.M., 1986, Duplex accretion and underplating in an ancient accretionary complex, Kodiak Islands, Alaska: Geology, v. 14, p. 160–163, doi: 10.1130/0091-7613(1986)14<160:DAAUIA>2.0.CO;2.

Sample, J.C., and Moore, J.C., 1987, Structural style and kinematics of an underplated slate belt, Kodiak and adjacent islands, Alaska: Geological Society of America Bulletin, v. 99, p. 7–20, doi: 10.1130/0016-7606(1987)99<7:SSAKOA>2.0.CO;2.

Schlocker, J., 1974, Geology of the San Francisco North Quadrangle, California: U.S. Geological Survey Professional Paper 782, 109 p.

Scholz, C.H., 2002, The Mechanics of Earthquakes and Faulting (2nd edition): Cambridge, Cambridge University Press, 471 p.

Secor, D.T., 1965, Role of fluid pressure in jointing: American Journal of Science, v. 263, p. 633–646.

Sibson, R.H., 1987, Earthquake rupturing as a hydrothermal mineralizing agent: Geology, v. 15, p. 701–704, doi: 10.1130/0091-7613(1987)15<701:ERAAMA>2.0.CO;2.

Sibson, R.H., 1989, Earthquake faulting as a structural process: Journal of Structural Geology, v. 11, p. 1–14, doi: 10.1016/0191-8141(89)90032-1.

Sibson, R.H., 1990, Conditions for fault-valve behaviour, *in* Knipe, R.J., et al., eds., Deformation, Mechanisms, Rheology, and Tectonics: London, Geological Society Special Publication, v. 54, p. 15–28.

Sibson, R.H., 1992, Implications of fault-valve behaviour for rupture nucleation and recurrence: Tectonophysics, v. 211, p. 283–293, doi: 10.1016/0040-1951(92)90065-E.

Sleep, N.H., and Blanpied, M.L., 1992, Creep, compaction and the weak rheology of major faults: Nature, v. 359, p. 687–692, doi: 10.1038/359687a0.

Swanson, S.E., and Schiffman, P., 1979, Textural evolution and metamorphism of pillow basalts from the Franciscan Complex, western Marin County, California: Contributions to Mineralogy and Petrology, v. 69, p. 291–299, doi: 10.1007/BF00372331.

Tchalenko, J.S., 1968, The evolution of kink-bands and the development of compression textures in sheared clays: Tectonophysics, v. 6, p. 159–174, doi: 10.1016/0040-1951(68)90017-6.

Van Gool, A.M., and Cawood, A., 1994, Frontal vs. basal accretion and contrasting particle paths in metamorphic thrust belts: Geology, v. 22, p. 51–54, doi: 10.1130/0091-7613(1994)022<0051:FVBAAC>2.3.CO;2.

Vannucchi, P., Maltman, A.J., Bettelli, G., and Clennel, B., 2003, On the nature of scaly fabric and scaly clay: Journal of Structural Geology, v. 25, p. 673–688, doi: 10.1016/S0191-8141(02)00066-4.

Vrolijk, P., 1990, On the mechanical role of smectite in subduction zones: Geology, v. 18, p. 703–707, doi: 10.1130/0091-7613(1990)018<0703:OTMROS>2.3.CO;2.

Wahrhaftig, C., 1984, Structure of the Marin Headlands block, California: A progress report, *in* Blake, M.C., Jr., ed., Franciscan Geology of Northern California: Pacific Section, Society of Economic Palaeontologists and Mineralogists Field Trip Guidebook, Pacific Section, v. 43, p. 31–50.

Wahrhaftig, C., 1989, Overview, *in* Wahrhaftig, C., et al., eds., Geology of San Francisco and vicinity: American Geophysical Union, International Geological Congress, Field Trip Guidebook T105, p. 1–5.

Wakabayashi, J., 1992, Nappes, tectonics of oblique plate convergence, and metamorphic evolution related to 140 million years of continuous subduction, Franciscan Complex, California: The Journal of Geology, v. 100, p. 19–40.

Wakabayashi, J., 1999, The Franciscan Complex, San Francisco Bay area: A record of subduction complex processes, *in* Wagner, D.L., et al., eds., Geologic Field Trip in Northern California: Geological Society of America Special Publication, v. 119, p. 1–21.

Manuscript Received 11 February 2005
Revised Manuscript Received 14 April 2006
Manuscript Accepted 2 June 2006

Printed in the USA

Figure DR1: Structural profile, measured across thrust dip, showing all of the major structural features recognized at the outcrop scale. Each “structural unit” is bounded by sheared contacts. Unit thickness, mean foliation, main structural features, and percentage of veins per area are also indicated.

DR1 - STRUCTURAL PROFILE MEASURED ACROSS THRUST DIP SHOWING MAJOR STRUCTURAL FEATURES AT MESO-SCALE